

DESIGN AND EVALUATION OF PIEZOELECTRIC SENSORS FOR THE MEASUREMENT OF BLOOD FLOW IN CORONARY IMPLANTS BY THE ULTRASONIC TRANSIT TIME METHOD

DISEÑO Y EVALUACIÓN DE SENSORES PIEZOELÉCTRICOS PARA LA MEDICIÓN DE FLUJO SANGUÍNEO EN IMPLANTES CORONARIOS POR EL MÉTODO DE TIEMPO DE TRÁNSITO ULTRASÓNICO

E. CARRILLO^{a†}, A. JIMÉNEZ^a, R. LÓPEZ^a, J. J. PORTELLES^b, L. F. DESDÍN^c

a) Instituto de Cibernética Matemática y Física (ICIMAF), CITMA, La Habana, Cuba; ernesto@icimaf.cu[†]

b) Facultad de Física, Universidad de la Habana, La Habana, Cuba.

c) Centro de Aplicaciones Tecnológicas y Desarrollo Nuclear, CITMA, La Habana, Cuba.

† corresponding author

Recibido 19/5/2020; Aceptado 00/00/2020

Nowadays, there is a small number of biomedical systems to verify the quality of coronary transplants. They are especially expensive and their closed architecture makes them impossible to reproduce. Based on the method known as Ultrasonic Transit Time Flow Measurement (TTFM), ultrasonic piezoelectric sensors useful to evaluate the quality of coronary implants during cardiovascular surgery were designed. They show repeatability in their parameters; produce a homogeneous acoustic field, an adequate acoustic intensity in their emission and allow a flow reading with an uncertainty below 5 ml/min. It is shown that the plastic known as Rexolite offers less acoustic attenuation and better mechanical coupling for the sensors compared to epoxy resin, attaining a better performance. These sensors operate together with an electronic module governed by a reconfigurable FPGA type platform. Finally, it is shown that time intervals in the order of tens of picoseconds can be detected by our sensor (i.e., flow rates smaller than 5 ml/min).

Internacionalmente existe un número escaso de sistemas biomédicos para verificar la calidad de los trasplantes coronarios, con elevados precios y una arquitectura muy cerrada, que imposibilita su reproducción. Basado en el método conocido como Tiempo de Tránsito Ultrasónico (TTFM), empleado para evaluar la calidad de los implantes coronarios durante la cirugía cardiovascular, se diseñaron y se desarrollaron sensores ultrasónicos piezoeléctricos TTFM que poseen una alta repetitividad en sus parámetros, producen un campo acústico homogéneo, una adecuada intensidad acústica en su emisión y poseen una incertidumbre de lectura inferior a 5 ml/min. Se concluyó que el material conocido como Rexolite brinda menor atenuación acústica y mejor acoplamiento mecánico respecto a la resina epóxica para el uso en sensores, lo que se traduce en una mejor prestación. Estos sensores operan conjuntamente con un módulo electrónico gobernado mediante una plataforma reconfigurable del tipo FPGA, permitiendo detectar intervalos de tiempo en el orden de las decenas de picosegundo (lo que equivale a flujos por debajo de 5 ml/min).

PACS: Medical uses of ultrasound (usos médicos del ultrasonido), 87.50.yt; piezoelectric devices (dispositivos piezoeléctricos), 85.50.-n; flow in cardiovascular systems (flujo en sistemas cardiovasculares), 47.63.Cb

I. INTRODUCTION

Smoking, obesity and a sedentary lifestyle are some of the factors that accelerate the occlusion processes in human coronary arteries, which constitutes one of the main causes of death worldwide [1]. When these occlusions become extreme, one of the most effective medical treatments to be applied is the implementation of coronary bypass implants, consisting in the placement of a grafted blood vessel parallel to the obstructed artery. The procedure substantially increases the life expectancy of individuals with high risk of heart attack.

One essential step in the coronary bypass surgery is to determine the value of the volumetric blood flow through the grafted vessel, which is an essential index to assess the quality of the implant: knowing it immediately indicates the effectiveness of the surgical procedure, and the eventual need to take correcting actions in order to avoid complications [2].

In spite of the good level of Cuban cardiovascular surgery,

up to now surgeons have confirmed blood circulation by just applying tactile pressure on the grafted vessel segment. It constitutes a rough, unreliable clinical procedure that strongly depends on the surgeon's experience. Obviously, it does not allow estimating the volume of blood per unit time circulating through the vessel [3,4].

Internationally, there is a small number of biomedical systems to verify the quality of coronary transplants, and their commercialization is monopolized by an U.S. company (MediStim). A typical system consists of a sensor and the measurement module. Each sensor can only be used around 10 times, and one surgery involves more than one of them. Eventually, the sensor can be sent to the company to be refurbished, which is an expensive process only affordable by developed countries.

Different techniques have been used in medical applications: electromagnetic flow meters [5], intraoperative arteriography

[6] and infrared ray angiography [7], constituting very invasive methods. The ultrasonic waves sensing method minimally affects the internal structure of the human body. Being a non-ionizing radiation, ultrasound is harmless to the internal structure of the body's cells. So, it has been intensively used in medicine, and experts agree that it will be used in the foreseeable future [8].

Ultrasound is used in two basic ways to measure blood flow: the Doppler technique and the Transit Time Flow Measurement Method (TTFM) [9]. The Doppler technique is used to detect obstructions and the assessment of the veins and arteries. The TTFM method allows quantifying the volumetric flow that circulates through a blood vessel in ml/min. The quality of coronary transplants is verified using both techniques.

In this article, which can be seen as a continuation of our previous work [10], the design and development of piezoelectric sensors, made of two different materials, is presented. Their design characteristics and measurement results are explained. The electrical signals produced by the sensors are conditioned and processed in an analog module, which allows measuring time intervals of tens of picoseconds, yielding a flow measurement uncertainty below 5 ml/min. Measurements of phase, resonance, anti-resonance, voltage and acoustic field are performed on the sensors in order to assess their performance within our system. The measurement moduli and the sensors constitute an inexpensive system, compared to similar equipment made by foreign firms, such as MediStim [11].

II. METHODS

II.1. Transit Time Flow Measurement (TTFM)

The ultrasonic Transit Time Method is based on the time the ultrasonic signal takes to propagate through a liquid (blood) travelling through a conduit (blood vessel), in favor or against the flow. The ultrasonic signal travelling against the flow, takes longer than the ultrasonic signal travelling in the same direction of the flow, assuming that the same route is followed in both cases.

The TTFM method is very accurate, even for the measurement of very small flows [11]. When an ultrasonic pulse is transmitted from a piezoelectric element (transmitter), it travels through the liquid medium and is received by another piezoelectric element (receiver). Then, the transmitter element becomes a receiver and the receiver element becomes a transmitter, repeating the cycle. Let us call t_d , the time ultrasound travels from one sensor to another, in favor of the flow, and t_i the time it travels against the flow. The difference $\Delta t = (t_i - t_d)$ depends only on the volumetric flow rate and does not depend on the propagation speed of the ultrasound in the medium, as illustrated in Fig. 1 [10].

II.2. Integrated System

Fig. 2 shows the basic block diagram of the blood flow measurement system in coronary vessels, whose description

and first results is the objective of this work. It is composed by the following parts [12]:

1. Ultrasonic bi-ceramic sensor.
2. Analog TTFM detection module.
3. Digital module for control and treatment.
4. Personal computer.

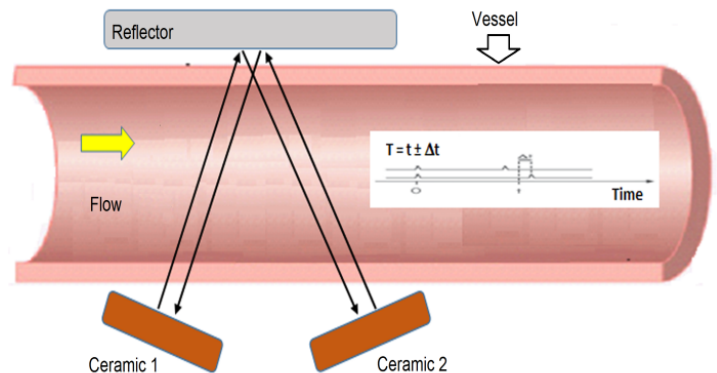


Figure 1. Scatter diagram of the variables voltage vs. flow in the phantom, Transit Time sensor measuring a blood vessel. (Adapted from [10]).

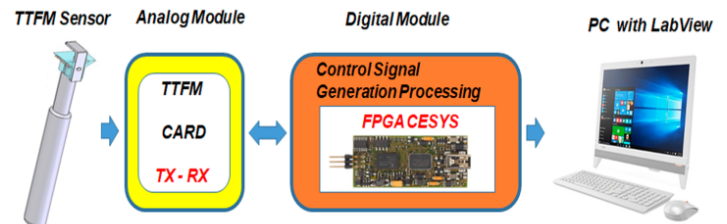


Figure 2. Block diagram of the TTFM system.

II.3. Analog module, digital module and A/D converter

The analog and digital moduli are presented in Fig. 3. They create the basic signals that provide the quantitative measurement of the volumetric blood flow. The process can be described in seven steps:

- a. The transmitter (Tx) is excited by two 2 MHz phase-inverted 15-pulse train, with a 3.3 V logic level. At the output, a 10 V (peak to peak) signal is obtained at low output impedance (2Ω).
- b. The Tx exciter signal is channeled alternately to each ceramic element through two analog switches, (SW1 and SW2). The echo signals received in both directions are applied to the receiver input (Rx) [13–15].
- c. Control signals 1 and 2 guarantee that while one piezoelectric ceramic emits an ultrasonic pulse, the other receives its reflected pulse, and vice versa.

- d. The phase detector compares the received 2 MHz pulse train with a 2 MHz master digital signal, producing at its output a pulse train with the same phase as the received train, but with a variable mark-to-space ratio, depending on the magnitude of the flow.
- e. The output of the phase detector is connected to a precision integrator, obtaining a voltage level proportional to the pulse duration [16]. This variable pulse train is sent to a precision integrator in the analog module, which converts phase (time) variations into voltage variations, with an uncertainty of $2 \mu\text{V}$, which is applied to an A/D converter. The accuracy of the measured time values is determined by the high resolution, 24-bit A/D converter used in the system (20-bit reliable). In addition, each flow measurement is made every 1 ms, therefore, a large data averaging is achieved, warranting a very reliable final reading.
- f. As a result, a serial 24-bit pulse train obtained from the A/D converter, is sent to a reconfigurable FPGA platform for further digital processing [17].

selected as 3 mm, its weight and easy handling are considered too.

Another important aspect in the design is the ability to withstand the sterilization process (360°C), which allows a larger reuse cycle that exceeds 10 measurements.

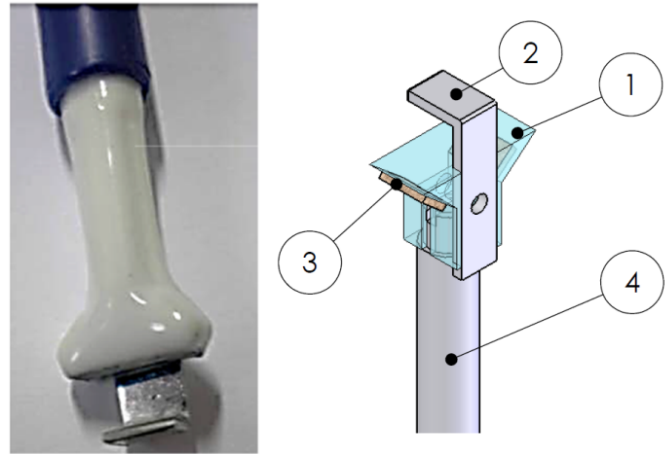


Figure 4. Structure of the TTFM sensor. Left panel: photograph of the real sensor. Right panel: sketch of the sensor; (1) wedge containing ceramic elements, (2) stainless steel reflector element, (3) two rectangular ceramic elements of 30 mm^2 area and (4) clamping rod.

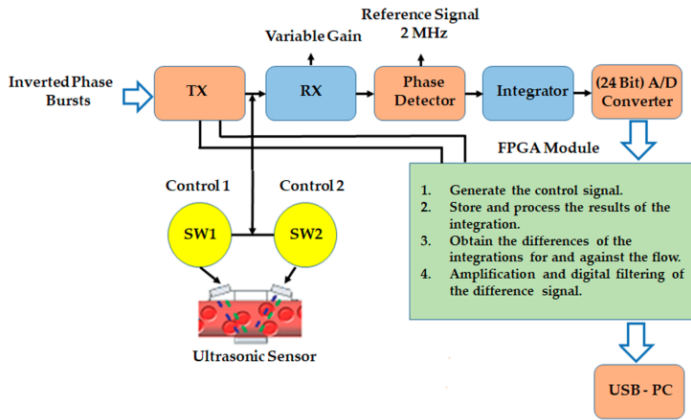


Figure 3. Block diagram of analog and digital moduli.

II.4. Ultrasonic TTFM sensor

The sensor is composed by two 2 MHz thickness mode rectangular piezoelectric ceramic elements, forming an angle. Both elements behave as transmitters and receivers alternately, i.e., if one element transmits, the other receives and vice versa. The measuring duct (vessel) is in the space between the ceramic elements and a metallic reflector. Then, the ultrasound crosses the duct four times per measurement. The ultrasonic sensor is composed of different parts, as shown in Fig. 4.

II.5. Design of TTFM sensors (determination of dimensions depending on the materials selection)

The dimensions of the sensors were calculated according to the used material, taking into account longitudinal waves, since the transverse waves in liquids are attenuated very quickly. Two alternative models are analyzed (model A and B). The distance between the coupling wedge and the reflector was

Model A

In this model, a Rexolite wedge is proposed with an isosceles trapezoidal shape, where ceramics are glued on the two non-parallel sides of the wedge, to determine the direction of the emitted (received) ultrasonic beam from (to) the wedge. These beams impact in the center of the reflector element (P blue rectangle), which reflects them toward the wedge again (toward the “receiving” ceramic).

To achieve this, the refractions occurring inside the wedge are taken into account (see Fig. 5). To calculate the dimensions of the wedge, the following data was considered: h_1 (wedge height), h (distance from the wedge to the reflector), d (piezoelectric ceramic size), θ (wedge angle), V_a (longitudinal wave speed in water) and V_c (longitudinal wave speed in the wedge material).

Equations for design:

$$\text{Wavelength in ceramics (mm)} = \frac{\text{Wave speed in ceramic (km/s)}}{\text{Frequency (MHz)}}, \quad (1)$$

$$\text{Ceramics thickness} = \frac{1}{2} \text{Wavelength in ceramics}, \quad (2)$$

$$\text{Thickness (mm)} \times \text{Frequency (MHz)} = \frac{1}{2} \text{Wave speed (km/s)}. \quad (3)$$

Incidence angle of ultrasound in water (Fig. 5):

$$a = \arcsin\left(\frac{V_a}{V_c} \sin \theta\right), \quad (4)$$

$$L = 2\left(a + \frac{P}{2} + c\right), \quad (5)$$

$$a = h \tan \alpha \cos^1 \theta,$$

$$P = \frac{d}{\cos \theta},$$

$$c = \frac{e}{\cos \theta},$$

$$e = d - \frac{h_1}{\sin \theta}.$$

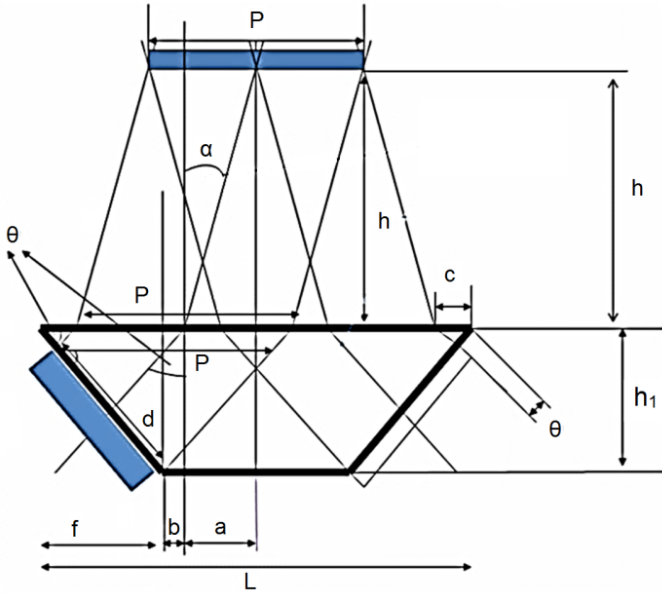


Figure 5. Scheme of the wedge's dimensions of TTFM sensors (Model A, Rexolite material). The reflector is represented as a blue rectangle on top, and only the left piezoelectric ceramic is shown, also represented as a blue rectangle.

Upper wedge length (Fig. 5):

$$L = 2h \tan \alpha + \frac{d}{2 \cos \theta} + \frac{d - h_1 / \sin \theta}{\cos \theta}, \quad (10)$$

$$b = \frac{L}{2} - a - f, \quad (11)$$

$$f = \frac{h_1}{\tan \theta}. \quad (12)$$

Lower wedge length (Fig. 5):

$$2(a + b) = L - \frac{2h_1}{\tan \theta}. \quad (13)$$

With equations (1 - 13), all wedge dimensions are obtained (according to Fig. 5). The value of h corresponds to a diameter greater than or equal to the characteristic diameter of arteries (of the order of 2-3 cm, depending on blood pressure) [11]. The value of h_1 will be taken according to the width of the wedge's bottom (larger than 6 mm) so that the design of the handle is the same for all sensors. The value of d will be 4.9 mm, with a P size (width of the reflector) capable of reflecting adequately the ultrasonic beam.

(6) Model B

This model has a wedge made with epoxy resin: the ceramics are glued to an acrylic support, and the remaining space is filled with epoxy resin, which forms the wedge (Fig. 6). The calculations for an epoxy resin wedge can be made using the equations below.

Height of the acrylic support (Fig. 6):

$$h_z = h_1 + g \cos \theta + k. \quad (14)$$

Outer length of the acrylic support (Fig. 6):

$$L_z = L + 2j = L + \frac{2g}{\sin \theta}. \quad (15)$$

End-to-end length of the Rexolite wedge (Fig. 6):

$$2i + 2(a + b) = 2g \sin \theta + L - \frac{2h_1}{\tan \theta}. \quad (16)$$

With equations (14 - 16), the geometric calculation can be made, obtaining the dimensions of the acrylic support to be implemented.

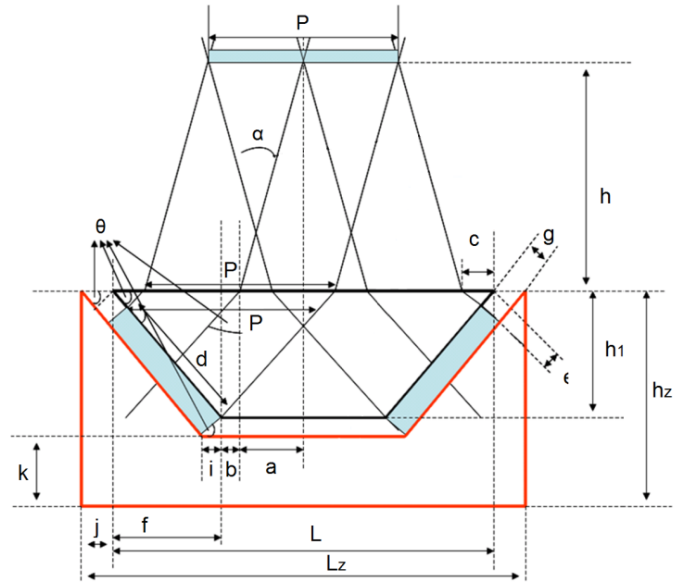


Figure 6. Scheme showing the dimensions of the TTFM sensors (Model B, epoxy resin material). The part indicated by red lines represents the acrylic support mentioned in the text.

Notice that g is the thickness of the piezoelectric ceramic element, and is related to the sensor's working frequency (see equations 1 and 2). h_z is the height of the acrylic support, L_z is the width of the acrylic support and j is the distance between the end of Rexolite wedge and the end of the acrylic support. The value of k is determined by the resistance selected in design, resulting in a value greater than 2 mm.

III. RESULTS FOR TTFM SENSORS (MODELS A AND B)

III.1. Results of TTFM sensors at 2 MHz working frequency

The design of sensors depends on an ultrasonic evaluation using the pulse-echo option, illustrated in Figs. 7 and 8. They show that the voltage amplitude for Rexolite is higher, in average, than that obtained for the epoxy resin (the difference

is as large as three-fold within the time interval from 90-100 μs). It represents a better performance in terms of material quality, with lower acoustic losses and higher sensitivity of the measurement system.

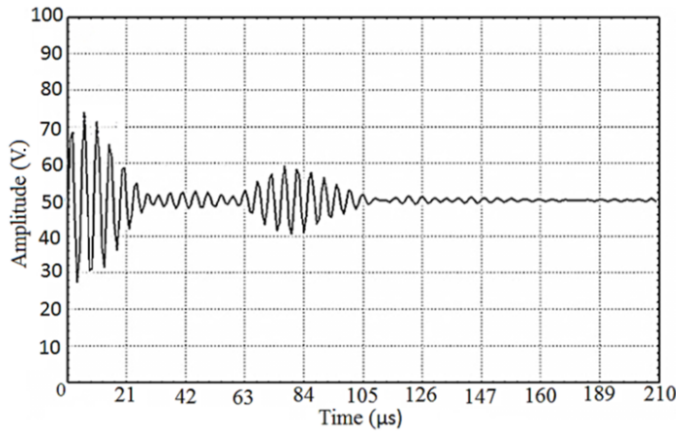


Figure 7. Average response of 3 mm, 2 MHz, epoxy resin TTFM sensors.

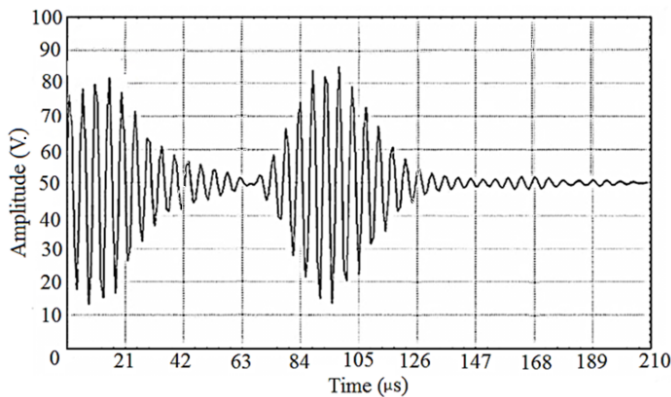


Figure 8. Average response of 3 mm, 2 MHz, Rexolite TTFM sensors.

It is worth noting that synchronization of images in Figs. 7 and 8 are different; because the materials under study have different acoustic properties.

III.2. Behavior of sensor's resonance frequency and phase

The TTFM sensors were designed to work at a frequency of 2 MHz, using two sensors for each model, as accounted in the color code of Figs. 9, 10 and 11. Using the Ultrascopie Omicrom Lab. (Bode 100) equipment, the resonance frequency, the phase values and the impedance module ($-Z-$) of the sensors were measured [18].

For the same resonance frequency (2 MHz), the Rexolite sensors show the highest electromechanical quality, as observed in Fig. 9. They have a lower phase shift compared to those built with epoxy, showing lower electromechanical losses and larger amplitude. Taking into account the elastic properties of Rexolite material, a better acoustic impedance coupling (sensor vs. human tissue) can be achieved and as a consequence, the pulse-transmission signal is improved.

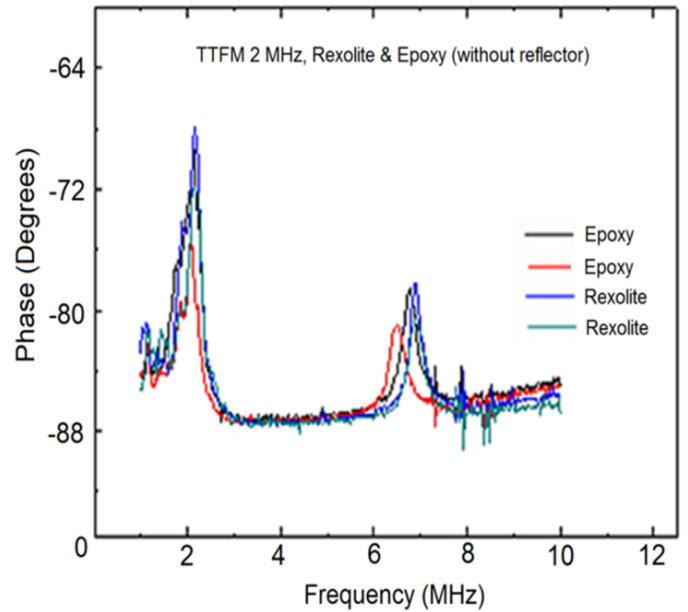


Figure 9. Phase behavior for 2 MHz TTFM sensors (models A and B).

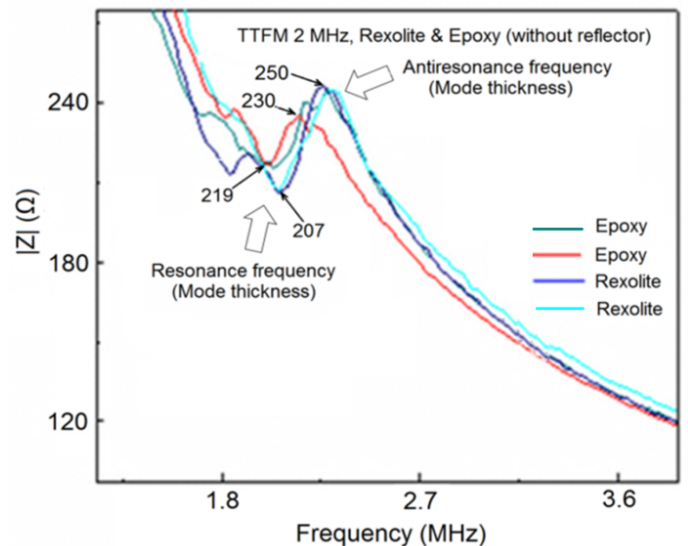


Figure 10. Impedance module behavior of 2 MHz TTFM sensors, (models A and B).

Rexolite has a lower value of serial impedance module at resonance frequency (207 Ω), higher value of parallel impedance module at antiresonance frequency (250 Ω) and lower electromechanical losses than Epoxy, see Fig. 10. Then, from now on, only results for Rexolite sensors will be presented.

III.3. Average response of sensors

The sensors made with Rexolite show higher voltage amplitude with respect to those made of epoxy. However, the transmission pulse response shows a similar behavior for all mounted sensors (model A and B), obtaining an average voltage variation of twice the maximum amplitude in both models.

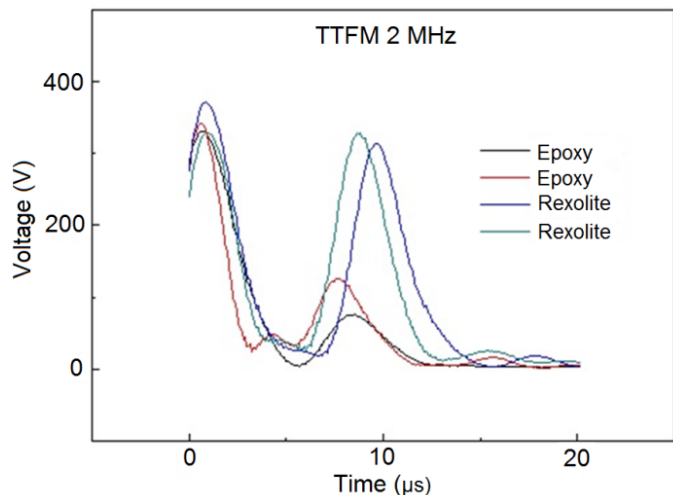


Figure 11. Pulse responses of the two materials used in the sensors (model A and B).

Thus, an acceptable repeatability for the application is obtained, see Fig. 11.

III.4. Results of the acoustic field measurement

The acoustic emissions of the 2 MHz TTFM sensors were evaluated and the radiation patterns were obtained using a calibrated hydrophone, in order to check construction procedure and repeatability. The cutting of the piezoelectric ceramics, the welding of the electrodes and the excitation data for this type of sensors, were taken into account. A 2 MHz 12-pulse train, an excitation voltage of 15 Vpp and a repetition frequency of 2 kHz, were chosen.

When both ceramics are excited at the same time, a maximum acoustic intensity is detected in a region centered around 4 mm in front of the sensor (within the A-B range), placing the hydrophone at the meeting point of both emissions (dot B), which is 1 mm away from the transducer, see Fig. 12.

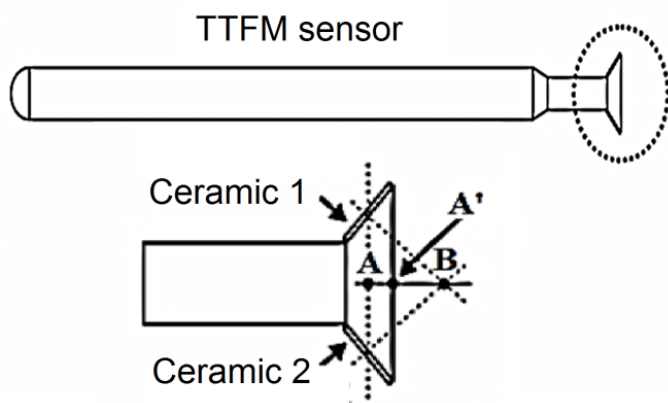


Figure 12. Range A-B of largest acoustic intensity of sensor emission (expected behavior).

The scanning of the space in front of the acoustic field generated by the sensors was done as illustrated in Fig. 13. A scan along the x-axis started at the upper left corner (seen

by the hydrophone facing the transducer). When it finished at the right extreme, a new x-scan started at the next y-value. Notice that the XY plane contains the point B (Fig. 12). The inter-planar distance was of 0.1 mm.

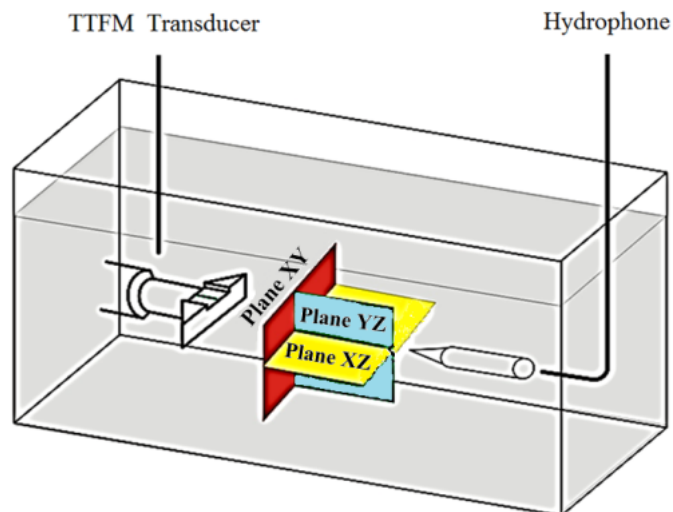


Figure 13. Configuration of the TTFM sensors and the hydrophone, showing the sweeping planes.

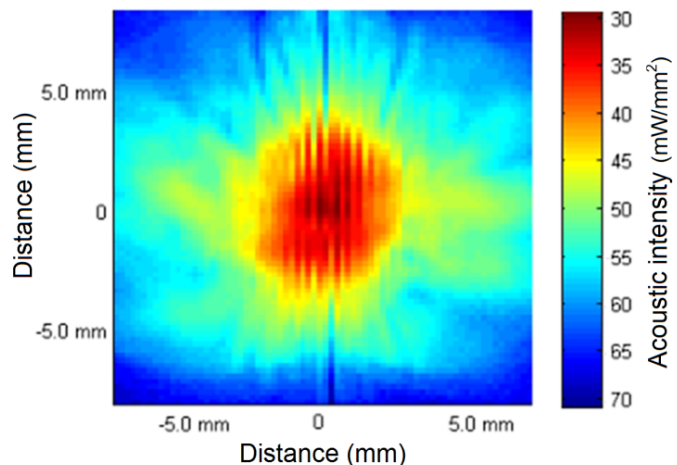


Figure 14. Acoustic intensity map on the X-Y plane for Rexolite ceramics (red plane in Fig. 13).

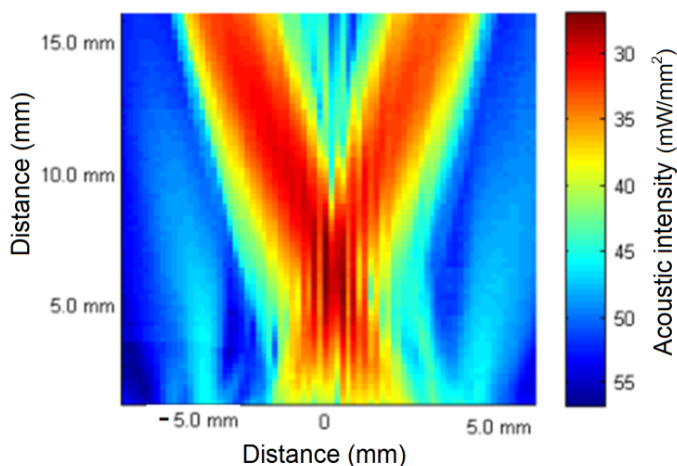


Figure 15. Acoustic intensity map on the XZ plane for Rexolite ceramics (yellow plane in Fig. 13).

From Figs 14 and 15, it can be concluded that 2 MHz TTFM sensors work correctly at a distance of 5.8 mm, they have a homogeneous near acoustic field that crosses through the artery to be measured. The crossed emissions of each ceramic are visible, which allows each of them to capture the incident signal coming from the reflector, emitted by both ceramics alternately. That is consistent with the physical principle of the ultrasonic transit time described earlier.

This behavior guarantees the construction and the repeatability in the building process of sensors, which includes equal cuts of the ceramic, equal mechanical supports and equal welding of the electrodes.

III.5. Flow measurement results using a pulsed flow phantom

The final validation of the results is mainly based on the flow measurements, through the use of a constant flow phantom that simulates blood circulation in an artery, see Fig. 16.

Through it, the operation of the sensor and the electronic module can be verified, which depends mainly on the used sensor. The phantom was filled with distilled water at room temperature (25 °C) [19].

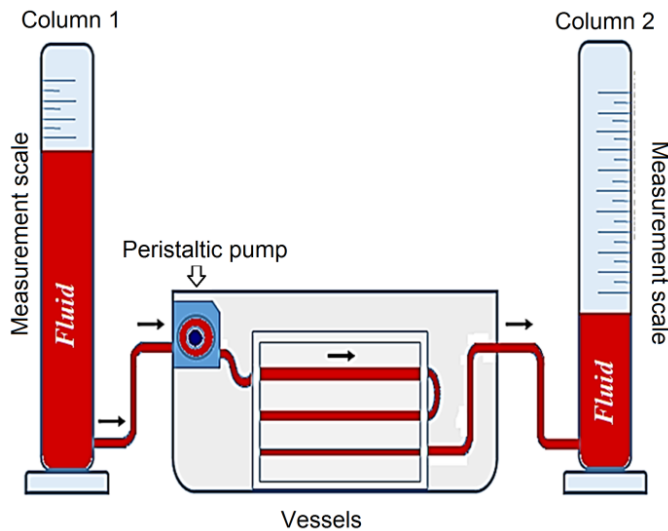


Figure 16. Schematic representation of the phantom able to produce a continuous flow (Peristaltic pump RS codes: 255-9605 and 330-834). The arrows indicate the direction of fluid motion.

Fig. 17 clearly indicates that the flow increases linearly as the voltage of the peristaltic pump increases. Therefore, a simple linear regression model was used to describe the relationship between the two variables. A summary of the results in the regression analysis and its corresponding model is shown in Table 1.

The high value of the Pearson correlation coefficient ($R = 0.999$) between the voltage and flow variables, means that there is a good correlation between them. On the other hand, the coefficient of determination indicates that 99% of the flow variation depends mainly on the uncertainty of the applied voltage, interpreted as a good measure of the fitting quality. The standard error indicates that, on average, the dispersion

of the observed values with respect to the values represented by the regression line is 1.022 ml/min.

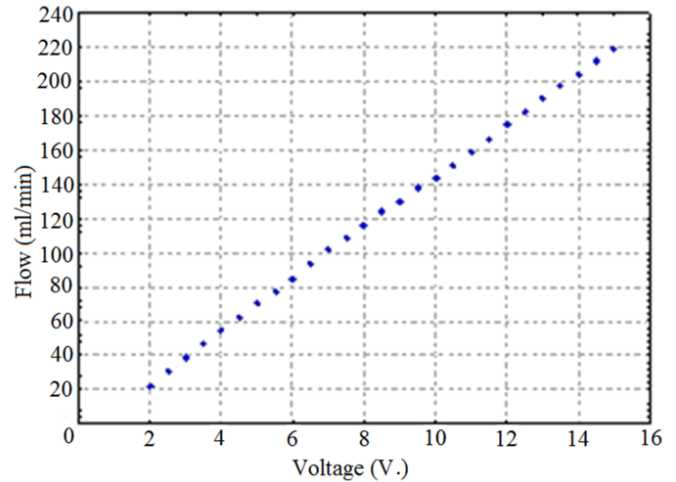


Figure 17. Scatter diagram of the variables voltage vs. flow in the phantom, considering all measurement made.

III.6. Flow measurement results using several sensors.

For the evaluation of the volumetric flow measurement system, three Rexolite 2 MHz ultrasonic sensors were used, named as: sensor 1, sensor 2 and sensor 3.

Table 1. Summary of regression analysis results (Fig. 17)

Model	Coefficients		t	P Value	Uncert. Coefficient 95 %	
	B	Stand. Error			Lower Limit	Upper Limit
Intercept	-5.515	0.519	-10.634	0.000	-6.584	-4.447
Voltage (V)	15.018	0.055	270.734	0.000	14.904	15.132
$R = 0.999$, $R^2 = 0.999$, Standard Error of Estimation = 1.022 V.						

Voltage measurements were made according to the flow values used in the phantom calibration [20,21].

The voltage measured at the analog module output, for each sensor, as a function of flow values controlled by the pump, is directly proportional to the volumetric flow. This voltage was measured at the A/D's output, using a logic analyzer with a resolution of 20 mV, so two sets of measurements were obtained for each sensor.

To study the relationship between the variable flow (ml/min) and the variable voltage (V.), a data dispersion diagram was constructed, in which each sensor is identified by its name, see Fig. 18.

These sensors behave slightly differently, thus obtaining three data sets, measured under the same conditions. The behaviors obtained depend on the sensor construction process and the inherent differences in each ceramic.

The values of blood flow measurements, validated in the medical practice are between 20-80 ml/min [1]. Therefore, a 95% linear regression model was performed for each sensor; considering that range of values, see Figs. 19, 20 and 21.

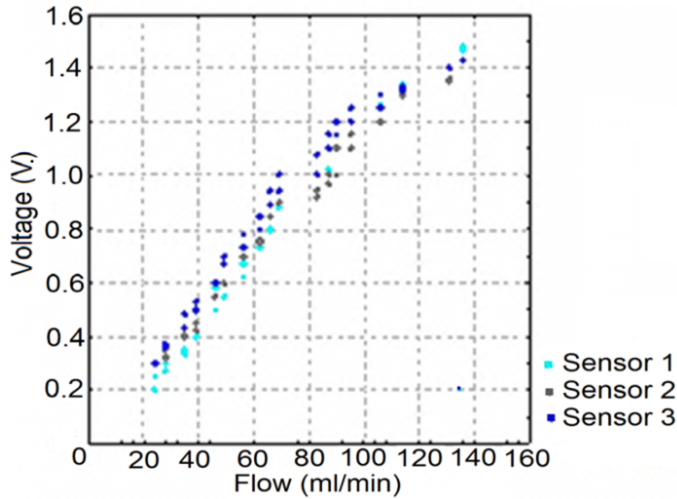


Figure 18. Data dispersion diagram of three Rexolite sensors, including all measurements.

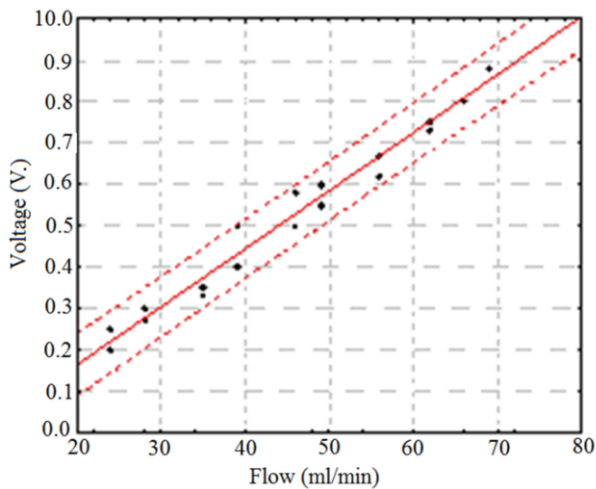


Figure 19. Rexolite sensor 1 regression diagram.

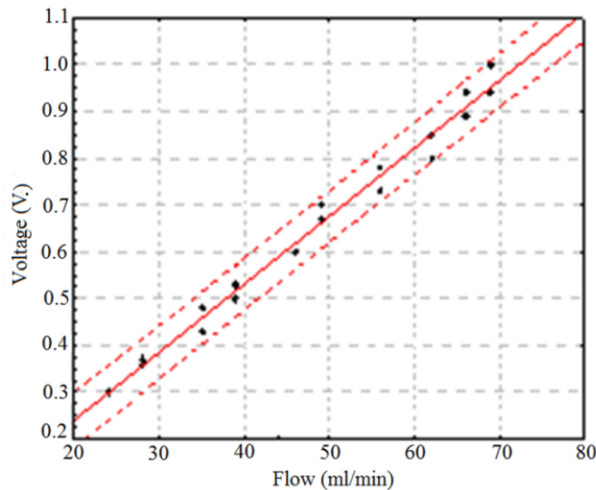


Figure 20. Rexolite sensor 2 regression diagram.

According to the results, a standard error of the predicted value of 2.4, 1.8 and 1.8 ml/min was obtained for the three sensors, respectively. The prediction error was calculated with a confidence of 95% for each flow value, based on measured average voltage levels. So, the predicted error for future measurements are: 5.0, 3.7 and 3.7 ml/min, respectively.

It consists of forecasts made in the medium term, with a time range between six months to three years, that is, errors occurring due to the continued use of the sensors [20].

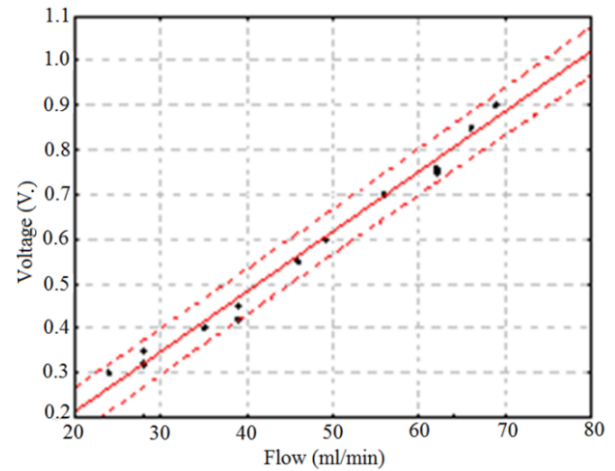


Figure 21. Rexolite sensor 3 regression diagram.

The minimum predicted values are lower than those reported by the commercial company MediStim, (5 ml/min) [11].

III.7. Implementation of LabView-based software (front panel designed for data presentation).

In order to visualize the blood flow signals and values, we designed an ad-hoc software (based on LabView). The front panel is shown in Fig. 22, where the blood flow signal can be visualized in real time, being updated constantly and stored during the signal acquisition, which is an advantage for the surgeon. It contains a Y axis scale showing the measured flow values expressed in ml/min. The time values associated with the measurements are indicated in the X axis. The REC key allows storing signal values during the desired period of time. In addition, some indicators are included: the flow average value (expressed in ml/min), the maximum and the minimum flow values, and the so-called Pulsatility Index (PI) [9]. Finally, the STOP key is included to stop the display of the signals and save the selected values.

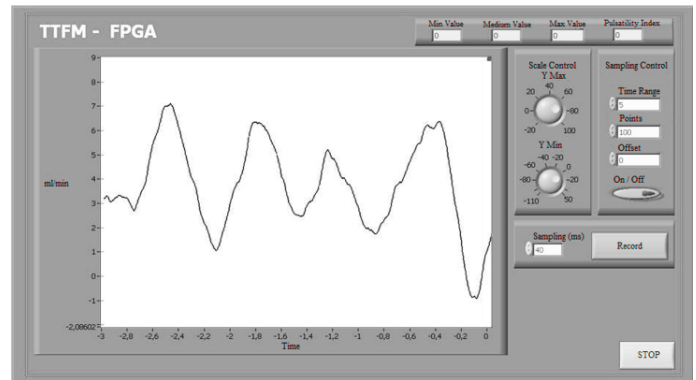


Figure 22. Front panel associated with the ad-hoc TTFM software.

IV. CONCLUSIONS

The basic aspects in the design of TTFM sensors are reviewed, considering the dimensions and the selection of materials

to be used. Two models were designed: model A (Rexolite wedge) and model B (epoxy resin wedge), which are the basic elements that allow flow measurements.

Both have high constructive repeatability, homogeneous acoustic field and allow a reading uncertainty lower than 5 ml/min. The Rexolite sensors provide larger acoustic intensity than the epoxy resin ones.

The resonance frequency and phase responses of the sensors were checked using the pulse transmission technique. Considering the dispersion of their values, the voltage difference of all sensors does not exceed twice the peak amplitude values, thus ensuring reading repeatability.

The flow measurement standard error was obtained for each of the three sensors with values of 2.39, 1.77 and 1.88 ml/min respectively, being smaller than those reported by similar sensors corresponding to the leader company (Medi-Stim), which is of 5 ml/min. The prediction error in the measurement, according to each sensor are: 5.02, 3.72 and 3.80 ml/min, respectively.

An analog module and a FPGA reconfigurable platform were implemented, capable of measuring time intervals of tens of picoseconds, allowing read errors of 5 ml/min.

The system as a whole was evaluated in a constant flow phantom.

ACKNOWLEDGMENTS

E. C.-B. thanks the “Abdus Salam” International Center for Theoretical Physics (Trieste, Italy) for a scholarship. The authors acknowledge the Department of Electrical Engineering, Bioelectronics Section, CINVESTAV (México D.F.) for support, and J. Prohías and A. Villar (“Hermanos Ameijeiras” hospital) for their valuable advice and help. We thank E. Altshuler for advise and suggestions.

V. REFERENCES

- [1] M. Gwozdziwicz. *Biomed. Papers* **148**, 59 (2004).
- [2] C. F. Barrera-Ramírez, J. Escaned. *Arch. Cardiol. Méx.* **75**, 335 (2005).
- [3] J.A. Finegold, P. Asaria and D.P. Francis. *Int. J. Cardiol.* **168**, 934 (2013).
- [4] J. Radcliffe. *Soc. Thoracic Surgeons.* **83**, 2251 (2007).
- [5] R. Tabrizchi and N. Iida, *Electromagnetic blood flow measurements*. In J. Moore and G. Zouridakis (Eds.). *Biomedical technology and devices handbook*, (CRC Press LLC, New York, 2003).
- [6] A. J. Room and D. Hoogerwerf, *J. Vascular Surg.* **16**, 239 (1992).
- [7] K. Kogure and E. Choromokos. *J. Appl. Physiol.* **26**, 154 (1969).
- [8] J. Seo and Y. -S. Kim. *Biomed. Eng. Lett.* **7**, 57 (2017)
- [9] D. P Taggart et al. *J. Thoracic Cardio. Surgery.* **159**, 1283 (2020).
- [10] A. Jiménez, E. Moreno, E. Carrillo and D. Torres, *Rev. Cubana Fis.* **28**, 4 (2011).
- [11] Medi-Stim. “Adding a New Dimension to Intraoperative Guidance”, *Catálogo Informativo*, (2017).
- [12] A. Ramos, H. Calas, L. Diez, E. Moreno, J. Prohías, A. Villar, E. Carrillo, A. Jiménez, W.C.A. Pereira, M.A. Von Krüger. *Physics Procedia.* **89**, 42 (2016).
- [13] Maxim, CMOS Analog Switches, MAX312/ MAX313/ MAX314. (2019) (www.maximintegrated.com/en/products/analog/analog-switches-multiplexers/MAX312.html).
- [14] Maxim, 35MHz, Ultra-Low-Noise Op Amps, MAX 4106/MAX4107. (2019) (www.datasheets.maximintegrated.com/en/ds/MAX4106-MAX4107.pdf).
- [15] Analog Devices, Low Noise, 90 MHz Variable-Gain Amplifiers, AD603. (2019) (www.analog.com/en/products/ad603.html).
- [16] BURR-BROWN, Low Noise, Dual SWITCHED INTEGRATOR, ACF2101. (2019) (www.it.com/BURR-BROWN, Low Noise, Dual SWITCHED INTEGRATOR, ACF2101, pdf).
- [17] EFM-02, Spartan-6LX FPGA module with USB 3.0. (2019) (www.cesys.com/en/our-products/fpga-boards/efm-02.html).
- [18] OMICRONLAB, ULTRASCOPE, User’s Manual. (2018) (www.omicronlab.com/documents.blackmagicdesign.com/UserManuals/BlackmagicUltraScopeManual.pdf).
- [19] M.A. Kruger and F.A. Martins. *Manual de Phantom de Flujo Sanguíneo, Versión 1.0.* (2007).
- [20] D. F. Cardona, J. L. González. *Inferencia estadística. Módulo de regresión lineal simple*, 1ra Ed. (Universidad del Rosario, 2013).
- [21] G. Cavada. *Rev. Chil. Endocrinol. Diabetes.* **6**, 127 (2013).

This work is licensed under the Creative Commons Attribution-NonCommercial 4.0 International (CC BY-NC 4.0, <http://creativecommons.org/licenses/by-nc/4.0>) license.

